Journal of Hydrology: Regional Studies 3 (2015) 125–138

Contents lists available at ScienceDirect

Journal of Hydrology: Regional Studies

journal homepage: www.elsevier.com/locate/ejrh

Temporal variability of precipitation in the Upper Tennessee Valley

James R. Jones [a,1], John S. Schwartz [b,*], Kelsey N. Ellis [c], Jon M. Hathaway [d], Curtis M. Jawdy [e]

[a] Department of Civil and Environmental Engineering, University of Tennessee, 411 John D Tickle Engineering Building, Knoxville, United States
[b] Department of Civil and Environmental Engineering, University of Tennessee, 413 John D Tickle Engineering Building, Knoxville, United States
[c] Department of Geography, University of Tennessee, Knoxville, United States
[d] Department of Civil and Environmental Engineering, University of Tennessee, 415 John D Tickle Engineering Building, Knoxville, United States
[e] River Operations Division, Tennessee Valley Authority, Knoxville, TN, United States

ARTICLE INFO

Article history:
Received 25 June 2014
Received in revised form 15 October 2014
Accepted 21 October 2014
Available online 6 January 2015

Keywords:
Precipitation trends
Temporal change point
Climate change
GCM down-scaling
Southern Appalachian region
Tennessee Valley Authority

ABSTRACT

Study region: Upper Tennessee River Basin, United States.
Study focus: The temporal variation of precipitation in the Upper Tennessee River Basin was investigated by utilizing datasets from the Tennessee Valley Authority (TVA) rain gauge network consisting of 56 rain gauges (1990–2010), and the National Weather Service (NWS) analyzing mean areal precipitation values for 78 subbasins (1950–2009). The Mann–Kendall trend test, Mann–Kendall–Sneyers test, Yamamoto Method, and Morlet's wavelet were applied to reveal precipitation trends and abrupt changes in annual precipitation volumes.
New hydrological insights for the region: Analyses indicated that: (a) 11% of the 78 subbasins experienced statistically significant increasing or decreasing precipitation over a 50-year period; (b) seasonal precipitation trends based on monthly volumes varied, with the summer and autumn series showing the largest significant increases; (c) abrupt changes in annual precipitation volumes were detected among subbasins corresponding to strong El Niño events; and (d) several subbasins displayed significant periodicities of 1, 6, 18, and 22 years in monthly volumes. These findings provide key information for regional precipitation down-scaling from global climate change models where the Appalachian mountainous terrain greatly impacts down-scaling results.
© 2014 The Authors. Published by Elsevier B.V. This is an open access article under the CC BY-NC-ND license (http://creativecommons.org/licenses/by-nc-nd/3.0/).

* Corresponding author. Tel.: +1 865 974 7721.
E-mail addresses: jjone149@utk.edu (J.R. Jones), jschwart@utk.edu (J.S. Schwartz), ellis@utk.edu (K.N. Ellis), jhathaw@utk.edu (J.M. Hathaway), cmjawdy@tva.gov (C.M. Jawdy).
[1] Present address: 200 Seitz Hall, Virginia Tech, 155 Ag Quad Lane, Blacksburg, VA 24081, United States.

http://dx.doi.org/10.1016/j.ejrh.2014.10.006
2214-5818/© 2014 The Authors. Published by Elsevier B.V. This is an open access article under the CC BY-NC-ND license (http://creativecommons.org/licenses/by-nc-nd/3.0/).

1. Introduction

Recent changes in climate have led to increased variability of the hydrological cycle at a global scale, creating uncertainty regarding predicting future climate conditions and associated impacts (Houghton et al., 1996). Perturbations in global climate models have created the need to study subsequent changes in hydroclimatic variables (e.g. rainfall, streamflow and evapotranspiration) to understand the regional effects of climate change. According to Karl et al. (2009), the southeast United States (US) has experienced an increase in extreme precipitation events and moderate to severe droughts in the 20th century. For instance, since the 1970s, moderate to severe droughts in the spring and summer months have increased by 12 and 14%, respectively. Ongoing efforts to model and project changes in extreme weather events in the eastern US have indicated that the southeast region should receive up to about 110 mm yr^{-1} more total extreme precipitation by the end of the 2050s (Gao et al., 2012), where extreme precipitation is defined as the 95th percentile of precipitation for days with accumulated precipitation greater than 1 mm. Furthermore, annual-mean precipitation is projected to increase over most of North America by 2030 (Solomon et al., 2007). Thus, understanding precipitation variability and extreme events associated with climate change is paramount to the ability of society to adapt to changes in water resource accessibility.

Most water storage reservoirs are planned, designed, and operated based on the historical pattern of water availability, quality, and demand under an assumption of constant climatic behavior (Westmacott and Burn, 1997; Abdul Aziz and Burn, 2006). The Tennessee River Basin contains the largest regulated river system in the southeast, and is managed by the Tennessee Valley Authority (TVA). There are 54 TVA-owned dams and reservoirs in this water storage control system. The reservoir system functions as an integrated, multipurpose operation with objectives to provide navigation, flood control, hydropower generation, recreation, and water quality. Since its inception, flood control has been the primary focus of TVA activities (Miller et al., 1998). Regionally, in recent years, several extreme precipitation events and their associated flooding have been the cause of large losses of life, and a source of large economic losses. For example, several days of heavy precipitation caused the Cumberland River at Nashville, Tennessee, to rise more than 10 m, cresting at 16 m in May 2010. In all, 26 people lost their lives and property damage estimates in the Greater Nashville area alone were over $2 billion (Hayes, 2011). The loss of property and life caused by weather-related disasters has increased awareness of the possibility that extreme events are a product of climate change (Easterling et al., 2000). For the Tennessee River Basin, precipitation is a vital component of system operation because of its influence on reservoir elevation levels and flooding, as well as the economic costs and benefits associated with hydropower generation. With respect to flood control, the eastern portion of the reservoir system is primarily planned to protect the city of Chattanooga, TN, from flooding. Keeping this objective in mind, it is necessary to conduct trend analyses to reveal precipitation variability and change point detection for future reservoir planning for the Upper Tennessee Valley; the corresponding drainage area to Chattanooga, TN.

Many studies have investigated hydrologic trends at various temporal scales in many parts of the world including precipitation and streamflow (Abdul Aziz and Burn, 2006; Akinremi et al., 1999; Cannarozzo et al., 2006; Chang and Kwon, 2007; Cheung et al., 2008; Costa and Soares, 2009; Gautam et al., 2010; Liang et al., 2011; Liu et al., 2008, 2009; Miller and Piechota, 2008; Partal and Kahya, 2006; Smith and Phillips, 2013; Yang et al., 2013; Zhang et al., 2000). Abdul Aziz and Burn (2006) explored trends and variability in the hydrological regime of the Mackenzie River Basin in northern Canada by utilizing the Mann–Kendall trend test on streamflow data spanning up to 87 continuous years. Noteworthy results include strong increasing trends over the winter month flows of December to April as well as increases in annual minimum flow. Furthermore, decreasing trends occurred in the early summer, late fall, and annual mean flows. Miller and Piechota (2008) found similar patterns in the Colorado River basin. With regards to the Tennessee River Basin, there has yet to be a comprehensive investigation of long-term trends in regional precipitation.

The main objectives of this study were to: (1) determine trends in precipitation at the annual and seasonal scales, (2) identify abrupt changes in annual precipitation totals in the Upper Tennessee Valley, and (3) investigate the periodicity of precipitation over the study area. TVA has a well-developed rain and stream gauge network for the entire Tennessee Valley and has gathered long-term climatic

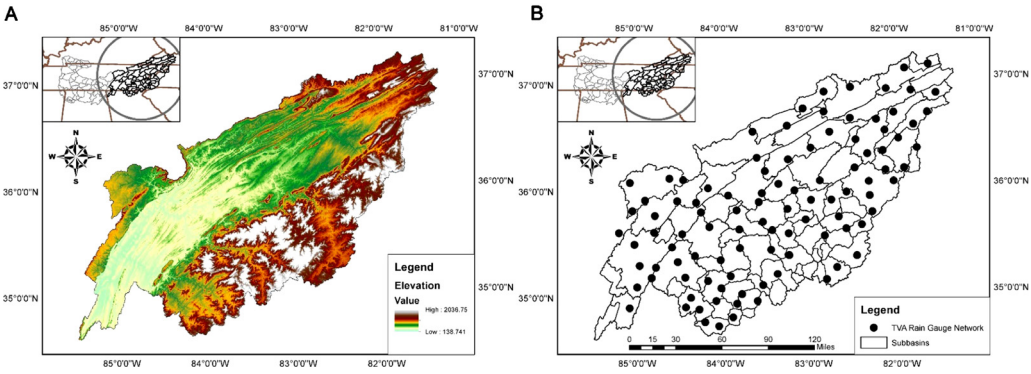

Fig. 1. Location maps showing (a) topography of study area, and (b) distribution of rain gauges for TVA Rain Gauge Network.

Table 1
Study design summary listing analysis tests and datasets associated with temporal scale and test objectives.

Analysis	Data used	Period(s) of record	Temporal scale	Objective
Trend analysis	TVA rain gauge network, subbasins	1990–2010, 1950–2009	Annual, seasonal	Quantify historical rainfall patterns
Change point detection	Subbasins	1950–2009	Annual	Reveal abrupt changes in precipitation
Wavelet analysis	Subbasins	1950–2009	Monthly	Determine periodicity of precipitation

and hydrologic data for river forecasting and hydrologic modeling purposes over a 65-year period, making such an analysis feasible.

2. Methodology

2.1. Study area

The Tennessee River Basin is composed of two fan-shape basins connected, in the vicinity of Chattanooga, TN, by a relatively narrow valley (Fig. 1a). The Upper Tennessee Valley lies between approximately 81° to 87° W and 34° to 38° N with altitudes ranging from 139 m to 2037 m. The region can be characterized as the 55,400 km^2 area upstream, or northeast of Chattanooga, which includes the slopes of the Blue Ridge and Great Smoky Mountains in the southern range of the Appalachian Mountains (Miller et al., 1998). The crest of the Great Smoky Mountains exceeds 1525 m for 55 km along the Tennessee-North Carolina State line, has 16 peaks that exceed 1829 m, and is the most massive mountain range east of the Mississippi River. Due to its high mountainous areas and deep valleys, the area has diverse topography which induces climate variation with differing altitudes. In general, average annual precipitation ranges from about 1016 mm (40 in.) for low-lying areas and up to 2286 mm (90 in.) for elevations greater than 1829 m (Hampson, 2000).

2.2. Study design

This study investigates the presence of trends, abrupt changes, and periodicity in precipitation over the Upper Tennessee Valley region by way of various statistical and mathematical techniques. The precipitation trends over several temporal scales are analyzed, including annual and seasonal periods, which were generated by monthly values. Analyses for abrupt changes and periodicity utilized the annual and monthly precipitation data, respectively (Table 1).

2.3. Precipitation datasets

Two datasets were compiled for temporal trend analyses; they included: (1) point measurements from the TVA gauge network for the period 1990–2010; and (2) 78 subbasin estimates derived from TVA data coupled with National Weather Service (NWS) for the period January 1950 through December 2009. Daily data were obtained from the TVA rain gauge network (Fig. 1b). Monthly data were compiled from daily data, and the annual and seasonal data were derived from monthly data. The period of record for these rain gauges is from 1990 to 2010. Rain gauge data extracted from the TVA rain gauge network were assessed for nonhomogeneity by utilizing the standard normal homogeneity test (SNHT) (Alexandersson, 1986) and the Buishand range test (Buishand, 1982). When the two tests rejected homogeneity, the time series were not used for analysis. This will ensure that detected trends are not caused by a change in observation times or relocation of the physical rain gauge. Noted in this study as the "subbasin" data and based on TVA and NWS data, developed mean areal precipitation values for the entire region used the Mean Areal Precipitation Program (MAP) created by the NWS River Forecasting Center (NWSRF). MAP uses pointy station data interpolated by the Thiessen Method. By using station metadata, any changes made to the rain gauge with respect to relocation and observation time was adjusted using double mass analysis.

2.4. Statistical trend analysis

Of the various statistical procedures used to analyze time series datasets, the nonparametric Mann–Kendall trend test is the most common (Zhang et al., 2006). This technique was first developed by Mann (1945), with Kendall (1975) deriving the distribution of the test statistic. Many hydrologic variables tend to exhibit a marked right skewness due to the influence of natural phenomena (Viessman and Lewis, 2003). The use of nonparametric techniques tends to be a more robust option when testing data which has departures from normality. Furthermore, the use of nonparametric techniques is known to be more resilient to outliers (Lanzante, 1996). In the Mann–Kendall trend test, the null hypothesis H_0 of the trend test is that there is no trend and that the data are random and independent; alternate hypothesis H_1 is that a trend is present in the time series. If $n \geq 10$ the test statistic can be approximated by the normal distribution, then the normalized test statistic Z_s can then be computed (Kendall, 1975). In a two-tailed test, $|Z_s| > Z_{\alpha/2}$ indicates that the null hypothesis has been rejected with α being the significance level of the test. For this study significance levels of 0.05 were utilized. The nonparametric estimate of the trend magnitude of the slope, β of linear trend, was taken to be the Theil–Sen's slope as proposed by Theil (1950) and Sen (1968). Theil–Sen's slope (β) is calculated as the median of all possible slopes.

The result of the Mann–Kendall can be biased by the effect of autocorrelation. The tendency for the null hypothesis to be falsely rejected at the specified significance level is increased when there is positive autocorrelation in the time series (von Storch and Navarra, 1999). Furthermore, if the data contain negative serial correlation then the significance of the trend can be underestimated (Yue and Wang, 2002). There have been several methods proposed for removing serial correlation. A common method is the use of "pre-whitening" on the original data set, and has been used by Douglas et al. (2000), Zhang et al. (2000, 2001), Burn and Hag Elnur (2002), and Yue and Wang (2002). The use of pre-whitening was suggested by von Storch and Navarra (1999) as a means to remove the influence of lag-1 serial correlation, but the method has shown the potential to remove a portion of the detected trend that can possibly lead to an inaccurate assessment of the significance of a trend (Shifteh Some'e et al., 2012; Wu et al., 2008; Yue and Wang, 2002). To adjust data for serial correlation the use of Trend-Free-Pre-Whitening (TFPW) was used (Yue and Wang, 2002). In this process the estimated trend, taken as Theil–Sen's slope, is removed from the series if the data series exhibits a trend greater than zero. Subsequently, to adjust for autocorrelation, the lag-1 serial correlation coefficient is removed from the detrended data series. After the removal of the serial correlation, the identified trend is added back to the dataset and the Mann–Kendall trend test is conducted on the adjusted time series (Novotny and Stefan, 2007). Yue and Wang (2002) describes this procedure in more detail.

2.5. Abrupt temporal changes in precipitation

2.5.1. Mann–Kendall–Sneyers test

The nonparametric Mann–Kendall–Sneyers test was utilized on the annual time series, which is a sequential version of the Mann Kendall rank statistic (Sneyers, 1990). Time series variables experience no change due to the null hypothesis assuming no trend in the data exists. Therefore, the time series could be stated as $x_1, x_2, \ldots, x_n$ (Liang et al., 2011). For each data point, x_i, the number of data points, n_i, of x_i preceding it ($i > j$) is computed such that $x_i > x_j$. The associated test statistic can be given by:

$$t_n = \sum_{i=1}^{N} n_i \tag{1}$$

t_n can be considered to be of normal distribution under the null hypothesis H_0 that a trend does not occur, and the mean and variance can be calculated by:

$$E(t_n) = \frac{n(n-1)}{4} \tag{2}$$

$$Var(t_n) = \frac{n(n-1)(2n+5)}{72} \tag{3}$$

The statistic $u(t)$ is given by:

$$u(t) = \frac{t_n - E(t)}{\sqrt{Var(t_n)}} \tag{4}$$

which is the forward sequence. Given that $u(t_1) = 0$, all $u(t_n)$ will result in a curve that will be designated as T_1. To search for an abrupt change in trend it is necessary to perform a similar analysis on the reverse data series. By applying this method a retrograde $u'(t)$ can be computed by:

$$u'(t_n) = -u(t_{i'}), \quad i' = (n+1) - i \tag{5}$$

for all $u'(t_n)$ and a curve designated as T_2 can be established. In the absence of a trend in the series, the graphical representation of $u(t)$ and $u'(t)$ will intersect several times; however, in the case of a significant trend the overlapping of the two curves, T_1 and T_2, within the specified confidence interval will allow for the beginning of a trend to be located. Moreover, if T_1 exceeds the confidence interval it can be determined that there is a significant upward or downward trend in the series (Fu and Wang, 1992). For this study the confidence interval was taken as ± 1.96 ($p = 0.05$).

2.5.2. Yamamoto method

The Yamamoto method can be used to detect a change point on a scale of several years by testing the significance between the means of two random samples of n size (Yamamoto et al., 1986). Given the reference year the signal to noise ratio (SNR) can be obtained as follows:

$$\text{SNR} = \frac{\left|\overline{x_1} - \overline{x_2}\right|}{s_1 + s_2} \tag{6}$$

where $\overline{x_1}$, $\overline{x_2}$, s_1, and s_2 are the mean and standard deviation of the data series before and after the reference year, respectively. In the present study the size of the subsets, n, is taken as 10. The t-statistic can be given by (Wei, 1999):

$$t = \frac{\left|\overline{x_1} - \overline{x_2}\right|}{s \times \sqrt{(1/n_1) + (1/n_2)}} \tag{7}$$

where s is defined as:

$$s = \sqrt{\frac{n_1 s_1^2 + n_2 s_2^2}{n_1 + n_2 - 2}} \tag{8}$$

Table 2
Minimum and maximum values of summary statistics for precipitation volumes (mm) in the annual and seasonal series for the 78 subbasins in the study area; period of record 1950–2009.

Variable	Subbasins		
	Median[a]	Mean[a]	95th percentile[a]
Annual precipitation	1069,1887	1088,1910	1349,2456
Spring precipitation	288,464	295,491	377,831
Summer precipitation	285,454	284,487	391,866
Autumn precipitation	195,409	219,459	338,841
Winter precipitation	243,483	257,489	366,725

[a] Minimum value for statistic, maximum value for statistic.

where n_1 and n_2 are the lengths of the respective samples. In this study the two samples were presumed to be the same length (i.e. $n_1 = n_2 = \mathrm{IH}$). By comparing the two equations above the following relationship can be derived:

$$t > \mathrm{SNR}\sqrt{\mathrm{IH}} \tag{9}$$

Furthermore, if IH = 10 SNR > 1.0 then $|t| > 3.162$, explicitly $t_\alpha = t_{.01} = 2.878$, and the significant trend at a 95% confidence interval can be obtained (Fu and Wang, 1992; Wei, 1999; Zhang et al., 2011).

2.6. Wavelet analysis

Many time series in hydrology display non-stationary in their statistics. The wavelet transform is a common tool used to reveal the periodic features of non-stationary variance at many different scales in time (Torrence and Compo, 1998). Moreover, it allows for the identification of the main periodicity in a time series and the progression in time of each frequency (Liang et al., 2011). The appropriate wavelet should have a similar pattern to the signal (Nakken, 1999), in which the Morlet wavelet function, as used herein, reveals peaks and troughs in wavelike signals in a fashion similar to rainfall data. Matlab wavelet package software provided by C. Torrence and G. Compo (http://atoc.colorado.edu/research/wavelets) was used in this study. The Morlet wave is given as follows:

$$\hat{\psi}_0(s\omega) = \pi^{1/4} H(\omega) e^{-(sw-\omega_0)^2/2} \tag{10}$$

where s is the wavelet scale, ω is the frequency, $H(\omega)$ is the Heaviside step function, $H(\omega) = 1$ if $\omega > 0$, $H(\omega) = 0$ otherwise; ω_0 is the non-dimensional frequency, taken to be 6 to satisfy the admissibility condition (Farge, 1992).

3. Results and discussion

3.1. Dataset descriptive statistics

Spatial resolution was good for the TVA rain gauge network data (1990–2010), but the available record length only extended 20 years. This infers that the power of the Mann–Kendall test may be poor (Burn and Hag Elnur, 2002). Therefore, the primary analysis utilized the longer term "subbasin" 1950–2009 dataset, however it did include a comparison to the 20-year TVA rain gauge network. For both datasets, the winter and spring series generally delivered the highest amounts of precipitation volumes while the summer and autumn series supplied less precipitation. (Tables 2 and 3). A general pattern that can be noted from the results was the decreasing of the winter and spring precipitation rates ($\mathrm{mm\,yr^{-1}}$), which were observed for both the TVA rain gauge network and subbasins in the study area. Conversely, the autumn and summer seasons experienced an increase in precipitation rates ($\mathrm{mm\,yr^{-1}}$) for both datasets (Tables 4–7).

Table 3
Minimum and maximum values of summary statistics for precipitation volumes in the annual and seasonal series for the TVA rain gauge network; period of record 1990–2010.

Variable	TVA Rain Gauge Network		
	Median[a]	Mean[a]	95th percentile[a]
Annual precipitation	807,1882	848,1836	1137,2227
Spring precipitation	222,469	234,476	293,674
Summer precipitation	214,470	216,449	301,642
Autumn precipitation	156,395	173,425	280,774
Winter precipitation	180,513	196,515	263,636

[a] Minimum value for statistic, maximum value for statistic.

Table 4
Summary of precipitation trends for the subbasins in the study area; period of record 1950–2009.

Variable	Number of decreasing trends	Number of increasing trends	Percent significant trends	Number of significant decreasing trends	Number of significant increasing trends
Annual precipitation	37	41	11	7	2
Spring precipitation	59	19	7	6	0
Summer precipitation	25	53	18	3	12
Winter precipitation	71	7	8	7	0
Autumn precipitation	16	62	20	2	15

Table 5
Summary of precipitation trends for the TVA rain gauge network; period of record 1990–2010.

Variable	Number of decreasing trends	Number of increasing trends	Percent significant trends	Number of significant decreasing trends	Number of significant increasing trends
Annual precipitation	30	26	0	0	0
Spring precipitation	43	13	4	2	0
Summer precipitation	13	43	14	0	8
Winter precipitation	54	2	20	11	0
Autumn precipitation	3	53	0	0	0

Table 6
Summary statistics of precipitation trends ($mm\,yr^{-1}$) for the subbasins in the study area; period of record 1950–2009.

Variable	Annual	Spring	Summer	Autumn	Winter
Mean trend	−0.50	−0.65	0.13	0.62	−0.75
Median trend	0.21	−0.40	0.29	0.62	−0.53
Minimum trend	−14.27	−4.15	−5.79	−2.42	−4.05
Maximum trend	5.04	0.97	1.58	3.15	0.56

3.2. Annual precipitation trends

Trends discovered for the annual series range from −14.27 to 5.04 $mm\,yr^{-1}$ for the period of record of 1950–2009 (Table 6). Annual precipitation decreased at 37 out of 78 subbasins (Table 4), and was more prevalent in the eastern portion of the study area with significant trends being distributed to

Table 7
Summary statistics of precipitation trends ($mm\,yr^{-1}$) for the TVA rain gauge network; period of record 1990–2010.

Variable	Annual	Spring	Summer	Autumn	Winter
Mean trend	−0.19	−2.06	2.62	3.17	−4.68
Median trend	−0.66	−2.29	2.64	3.05	−4.92
Minimum trend	−14.97	−7.59	−5.08	−1.81	−9.09
Maximum trend	13.26	4.92	10.22	10.71	1.07

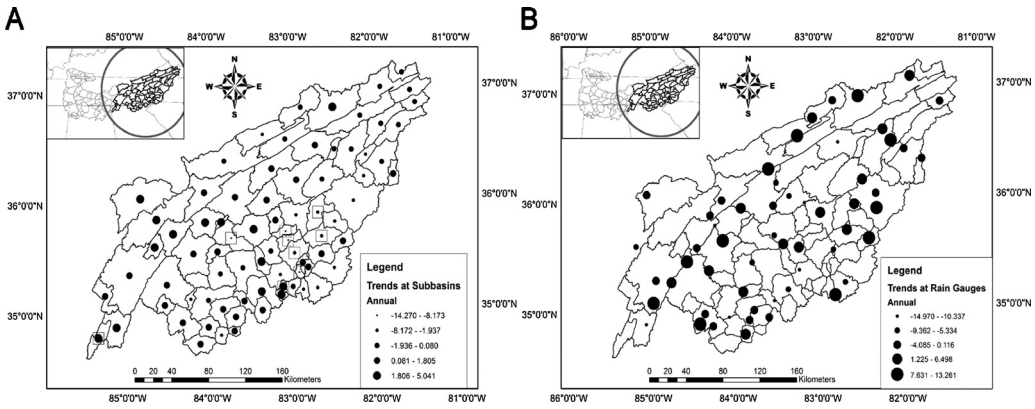

Fig. 2. Annual precipitation trends for (a) annual precipitation trends among subbasins; period 1950–2009; and (b) annual precipitation trends at TVA Rain Gauge Network; period 1990–2010. *Note*: *square denotes significance at the 95% confidence level.

the north of latitude 35° N (Fig. 2). The highest decreasing trend was detected at subbasin TWNT1 (−83.62° W, 35.62° N). Increasing trends were detected in 41 of the subbasins, and many were located on either side of the Appalachian mountain range (Table 4). A significant increasing trend was only identified for 2 subbasins; with the highest increasing trend being measured at TKRN7 (−83.13° N, 35.23° W). In comparison to trends of the TVA rain gauge network, the highest magnitude decreasing trends compare well on a spatial level with that of the rain gauges; however, the highest magnitude increasing trends found in the rain gauges varies from that of the subbasins. There appears to be good agreement with regard to trends found in the Appalachian Mountains with both series demonstrating decreasing trends.

The Intergovernmental Panel on Climate Change's (IPCC's) Fourth Assessment Report (AR4) concluded that precipitation has generally increased over latitudes north of 30° N over the period of 1900–2005 (Stocker et al., 2013). This is not consistent with the findings of the current study, which indicates similar amounts of increasing and decreasing trends. It should be noted that many of the significant decreasing trends were discovered in the eastern portion of the study area where the Appalachian Mountains are located. It is not surprising that the Appalachian Mountains are showing different trends than surrounding areas as evident by past studies (Li et al., 2013). Earlier studies have shown that the mountains disrupt large-scale flow, causing different interactions with major climate oscillations as compared to other areas. El Niño, the warm anomaly in the equatorial Pacific, is associated with wetter and cooler than normal conditions across most of the southeast, while La Niña, the cold anomaly in the equatorial Pacific, is tied to unseasonably dry and warm conditions; however, these effects are not as profoundly observed through portions of the Appalachian plateau (Budikova, 2008; New et al., 2001). Also, Konrad (1994) shows the northeast–southwest oriented Appalachian Mountains alter the lower tropospheric circulation pattern in ways that encourage heavy rainfall in some areas (notably the southern and southeastern slopes), while blocking moisture transport and prohibiting heavy rainfall in other areas. Thus, for the current study focusing on the Appalachian Mountains, different temporal trends can be expected as compared to the remainder of the southeast region and within the study area itself, due to varying impacts of large-scale oscillations and local forcing mechanisms. Although the IPCC's analysis of global climate change trends is important, regional weather patterns should be considered critical to local climates in the future.

3.3. Seasonal precipitation trends

For the selected subbasins and rain gauge data in the study area, the Mann–Kendall trend test was applied to detect the temporal trends of the seasonal precipitation time series. All significant trends detected in the spring and winter precipitation series were negative (Tables 4 and 5). Moreover, when

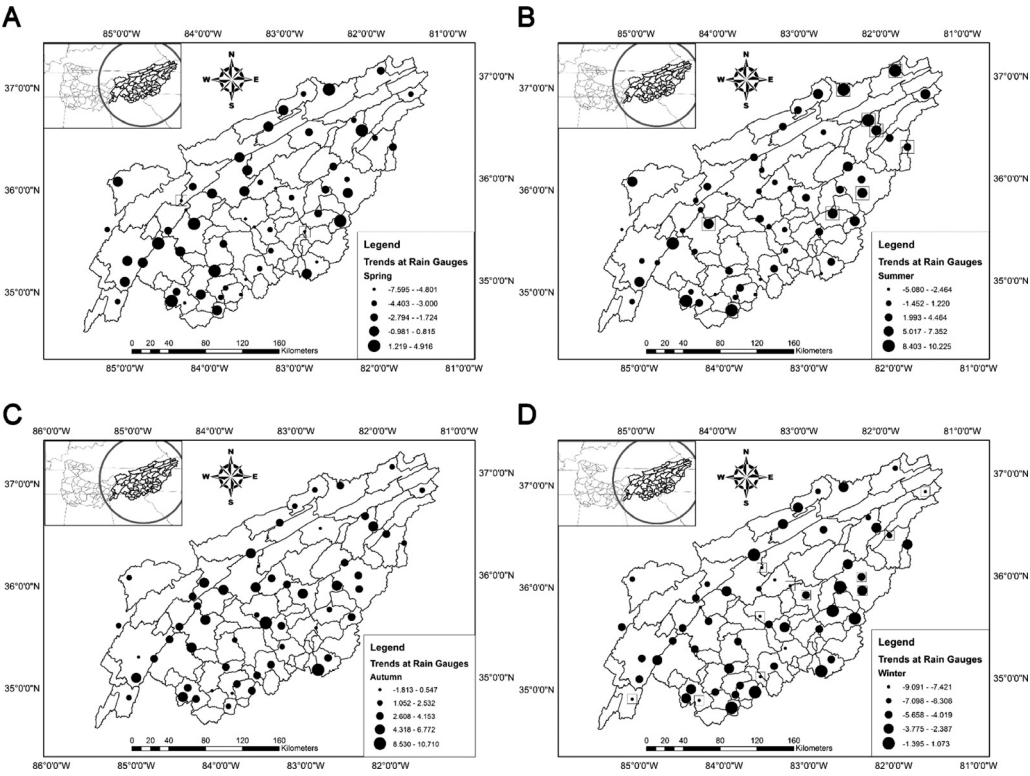

Fig. 3. Precipitation trends (mm yr^{-1}) among subbasins for (a) spring, (b) summer, (c) autumn, and (d) winter. *Note*: *square denotes significant at the 95% confidence level.

considering all of the subbasins, for the spring and winter seasons, the range of values are −14.27 to 5.04 and −4.05 to 0.56 in mm yr^{-1}, respectively. Fig. 3a illustrates the spatial distribution of subbasin trends for the spring series. Similar to that of the annual series, many of the decreasing trends detected for the spring series were present in the eastern portion of the study area, while many of the positive trends were in the central to western portion of the region. There were negative and positive trends detected in the summer and autumn time series; however, there were overall more decreasing trends discovered for both seasons. As seen in Fig. 3b and c, more subbasins exhibited increasing trends in the higher elevations in the Appalachian Mountains for the autumn and summer series. Furthermore, as noted in Table 4, many of the significant trends were increasing for the summer and autumn seasons. This general pattern observed with the subbasins was in good agreement with that of the rain gauge data (Fig. 4).

The increase of precipitation rates (mm yr^{-1}) in the summer and autumn series for the subbasins in the study area were indicative of less frequent continental fronts (with their associated large precipitation volumes) coupled with intensification of summer and autumn storms. Year-to-year fluctuations in summer precipitation variability have intensified over the southeast US (Li et al., 2011; Wang et al., 2010). Li et al. (2011) revealed that the North Atlantic Subtropical High (NASH), which has become more intense with respect to movement in the last 30 years, is migrating westward; while its movement north and south has been enhanced. Li et al. (2011) suggested that the intensification and westward drift of NASH has caused the frequency of summer variability to more than double compared to the previous 30 years. Our results suggest that while the Appalachian Mountains have an obvious impact on local precipitation, the intensification of summer rainfall variability in this area was similar to that experienced by the region as a whole.

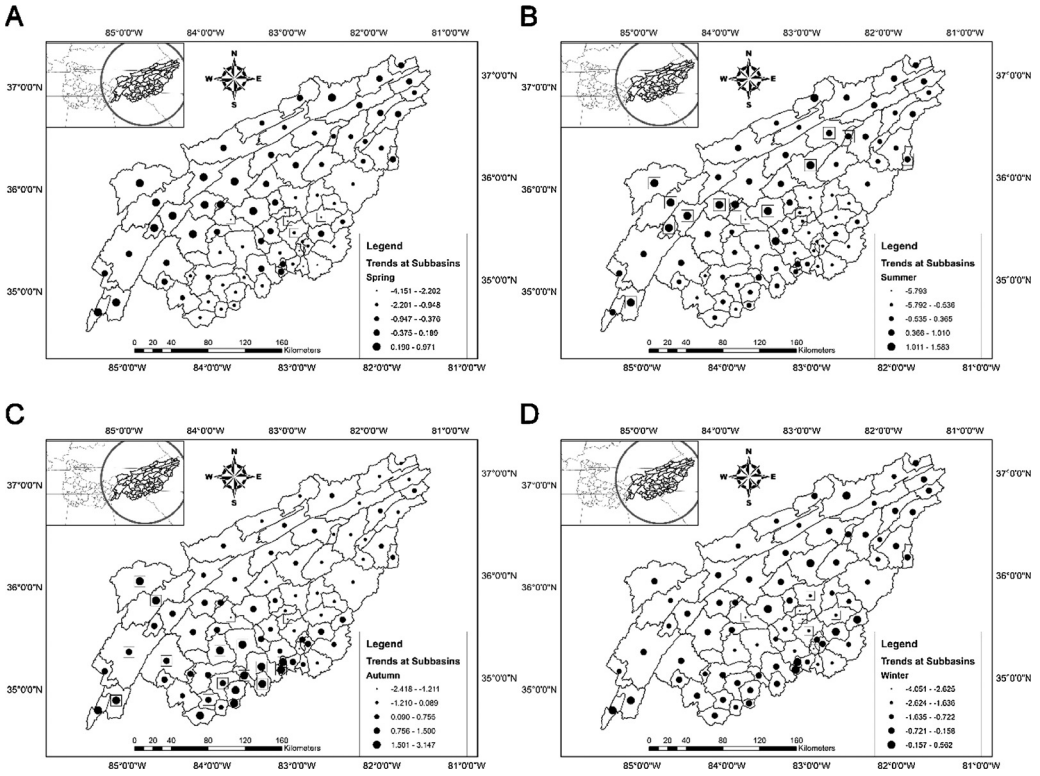

Fig. 4. Precipitation trends (mm yr^{-1}) for the TVA rain gauge network for (a) spring, (b) summer, (c) autumn, and (d) winter. *Note*: *square denotes significant at the 95% confidence level.

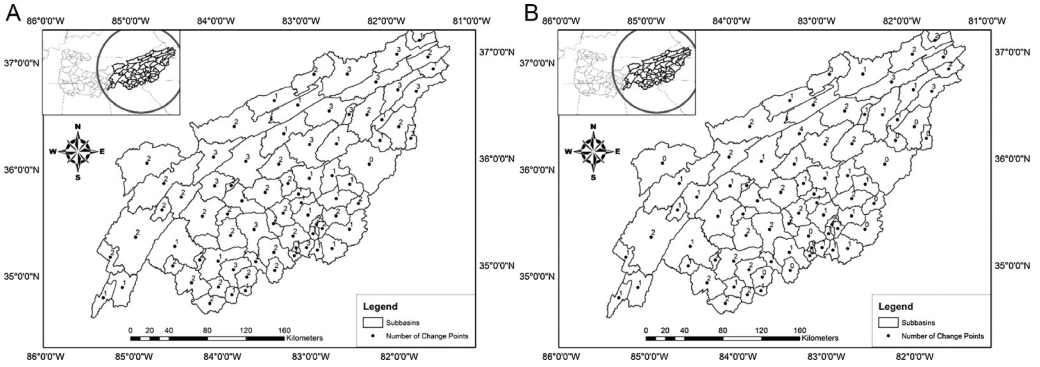

Fig. 5. Number of change points for subbasins; period of record 1950–2009 for (a) number of change points detected using the Mann–Kendall–Sneyers method, and (b) number of change points detected using the Yamamoto method.

3.4. Abrupt changes in precipitation

Fig. 5a and b shows the distribution of abrupt changes in annual precipitation (change points) in the study area for the Mann–Kendall–Sneyers test and Yamamoto method, respectively. Based on the Mann–Kendall rank statistic, the graphical analyses for the annual precipitation were applied to curves T_1 and T_2 of 78 subbasins to identify the intersection of the two curves and determine a year

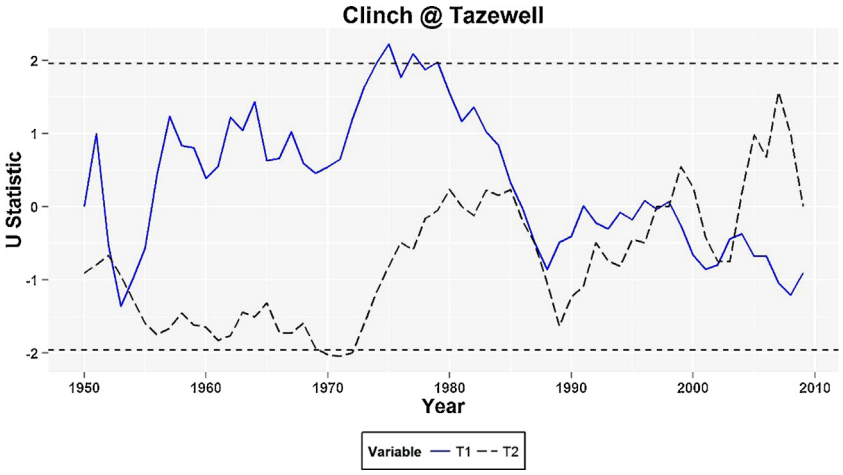

Fig. 6. Change points using Mann–Kendall–Sneyers test for subbasin TAZT1; period 1950–2009.

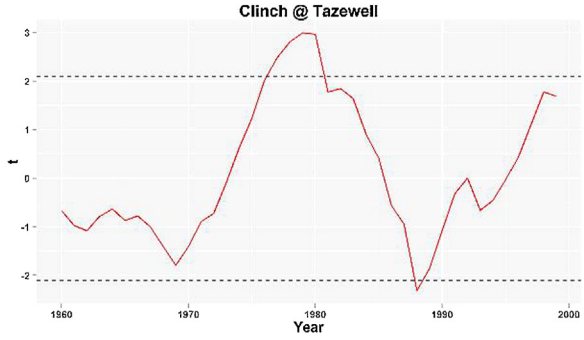

Fig. 7. Change points using Yamamoto method test for TAZT1; period 1950–2009.

of change. The subbasin TAZT1 (−83.07° W, 34.56° N) was selected as an example to demonstrate the abrupt change occurring in the annual precipitation series. The Mann–Kendall–Sneyers test results in Fig. 6 show that two abrupt changes occurred in 1953 and 1988, showing increasing and decreasing precipitation changes, respectively. Fig. 7 also provides the results for the Yamamoto method with respect to the annual series of TAZT1. Two change points were detected and took place between 1978–1980 and 1988. In many cases, the number of change points and the associated year of change for a given basin were similar to its respective neighbors. Furthermore, the number of change points detected in subbasins throughout the area ranged from zero to four. There have been several studies that detected and investigated El Niño events by several different means (Cane, 1983; Frappier et al., 2002; Jin et al., 2003), and this study revealed that many change points corresponded with a number of reported events. For instance, one of the stronger El Niño events (1982–1983) was a common change point detected throughout the study area. This suggests that the variability may be due to large scale oscillation rather than long term climate variability.

Since abrupt changes detected by the Mann–Kendall–Sneyers test, by nature, reflect a significant change in trend for the given series, and those by the Yamamoto method indicate a significant change in the average of two samples, the results may not be consistent (Liang et al., 2011). Although for this particular basin, the two methods were consistent with respect to the change point detected in 1988, and in many instances throughout the region the two techniques were in good agreement.

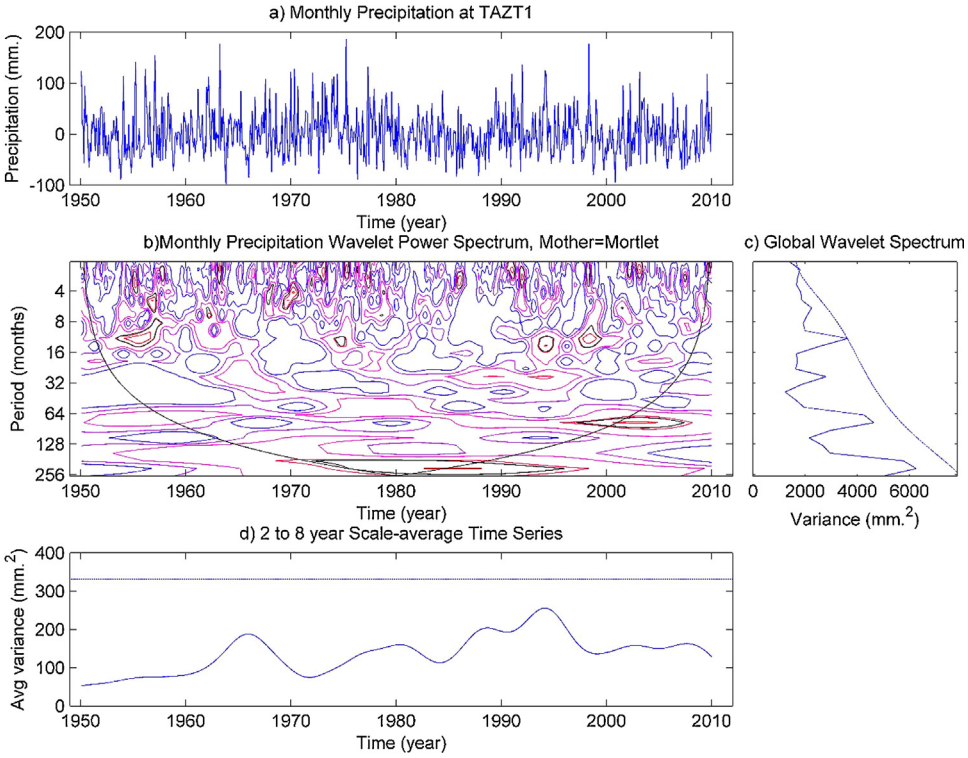

Fig. 8. Wavelet analysis results showing (a) anomaly of the monthly precipitation time series of TAZT1 for the period of 1950–2009; (b) the wavelet power spectrum (power contour levels are 75%, 50%, 25%, and 5%); (c) the global wavelet power spectrum (dashed line is the 95% confidence line); and (d) the scale-average wavelet power for a 2–8 year band (dashed line represents the 95% confidence line).

3.5. *Wavelet analysis*

The monthly precipitation series for subbasins in the study area were measured using the Morlet wavelet transform to elucidate precipitation periodicity, allowing an understanding of the frequencies of rainfall patterns. Fig. 8 displays the period detection result for TAZT1 in the 65 year period studied for the Upper Tennessee Valley. The means for the entire record have been removed to define an anomaly series to compare with previous studies. The monthly standardized anomaly series for TAZT1 can be found in Fig. 8a. Throughout the period, the variance shown in the 2–8 year band is below the 95% confidence limit (Fig. 8d). For TAZT1, the period of 1 year which is significant at the 95% confidence level, indicated a strong annual signal. It can be noted that many periods exist where there is significant power; however, these periods are within the cone of influence and should not be considered. Throughout the region, there exist periods of 1, 6, 18, and 22 years which were significant. Historical records of precipitation and temperature in the southeast US reveal much interannual and interdecadal variability, which agrees well with the findings of this study (Ingram et al., 2013).

4. Conclusion

The annual precipitation series with a period of record of 1950–2009 displayed positive and negative trends at 52 and 48% of the subbasins, respectively. Only seven negative and two positive trends were observed to be significant at the 95% confidence level, and ranged from −14.27 to 5.04 mm yr^{-1}, respectively. The distribution of the annual trends varied due to topographically induced climate variations with decreasing trends being concentrated in the Appalachian Mountain region, primarily located in the eastern area of the Upper Tennessee River Basin.

Both negative and positive trends were observed in seasonal precipitation. The trends in the spring and winter series were mostly negative, while trends in autumn and summer were generally increasing. This pattern was observed for both rain gauge and subbasin data series. The strongest negative trend found in all seasonal series for the subbasins occurred in the summer with a trend of $-5.79\,\mathrm{mm\,yr^{-1}}$. Further, the highest increasing trend occurred in autumn with a precipitation increasing at a rate of $10.71\,\mathrm{mm\,yr^{-1}}$.

Previous studies have concluded that El Niño phenomena as well as the NASH may have some impact on precipitation in the southeast US. It has also been recognized that the transport of moisture across the Appalachian Mountains adheres to different physical mechanisms. The results of this paper suggest that there are various trends occurring in the Upper Tennessee Valley, but further study is required to determine if the region is facing long-term climatic trends or short term climate variability due to impacts observed by El Niño. Moreover, due to the varying topography in the region, spatial analysis is needed to determine the degree of homogeneity of precipitation trends over the study area. It is recommended that future studies include the investigation of other hydroclimatic variables such as streamflow and evapotranspiration for the study area and the entire Tennessee Valley. Such information will allow more informed regional planning and management of water resources and infrastructure.

Acknowledgements

The study was financially supported by a grant through the Institute of a Secure and Sustainable Environment (ISSE), the University of Tennessee, Knoxville, United States. We appreciate the support from Dr. Chris Cox, ISSE Director. We also appreciate the assistance from the Tennessee Valley Authority, United States with database management.

References

Abdul Aziz, O.I., Burn, D.H., 2006. Trends and variability in the hydrological regime of the Mackenzie River Basin. J. Hydrol. 319 (1), 282–294.
Akinremi, O., McGinn, S., Cutforth, H., 1999. Precipitation trends on the Canadian Prairies. J. Clim. 12 (10), 2996–3003.
Alexandersson, H., 1986. A homogeneity test applied to precipitation data. J. Climatol. 6 (6), 661–675.
Budikova, D., 2008. Effect of the Arctic Oscillation on precipitation in the eastern USA during ENSO winters. Clim. Res. 37 (1), 3 (Open Access for articles 4 years old and older).
Buishand, T.A., 1982. Some methods for testing the homogeneity of rainfall records. J. Hydrol. 58 (1), 11–27.
Burn, D.H., Hag Elnur, M.A., 2002. Detection of hydrologic trends and variability. J. Hydrol. 255 (1), 107–122.
Cane, M.A., 1983. Oceanographic events during El Niño. Science 222 (4629), 1189–1195.
Cannarozzo, M., Noto, L.V., Viola, F., 2006. Spatial distribution of rainfall trends in Sicily (1921–2000). Phys. Chem. Earth A/B/C 31 (18), 1201–1211.
Chang, H., Kwon, W.-T., 2007. Spatial variations of summer precipitation trends in South Korea, 1973–2005. Environ. Res. Lett. 2 (4), 045012.
Cheung, W.H., Senay, G.B., Singh, A., 2008. Trends and spatial distribution of annual and seasonal rainfall in Ethiopia. Int. J. Climatol. 28 (13), 1723–1734.
Costa, A.C., Soares, A., 2009. Trends in extreme precipitation indices derived from a daily rainfall database for the South of Portugal. Int. J. Climatol. 29 (13), 1956–1975.
Douglas, E., Vogel, R., Kroll, C., 2000. Trends in floods and low flows in the United States: impact of spatial correlation. J. Hydrol. 240 (1), 90–105.
Easterling, D.R., et al., 2000. Climate extremes: observations, modeling, and impacts. Science 289 (5487), 2068–2074.
Farge, M., 1992. Wavelet transforms and their applications to turbulence. Annu. Rev. Fluid. Mech. 24 (1), 395–458.
Frappier, A., Sahagian, D., González, L.A., Carpenter, S.J., 2002. El Nino events recorded by stalagmite carbon isotopes. Science 298 (5593), 565.
Fu, C., Wang, Q., 1992. The definition and detection of the abrupt climatic change. Sci. Atmos. Sinica 16 (4), 482–493 (in Chinese).
Gao, Y., Fu, J., Drake, J., Liu, Y., Lamarque, J., 2012. Projected changes of extreme weather events in the eastern United States based on a high resolution climate modeling system. Environ. Res. Lett. 7 (4), 044025.
Gautam, M.R., Acharya, K., Tuladhar, M.K., 2010. Upward trend of streamflow and precipitation in a small, non-snow-fed, mountainous watershed in Nepal. J. Hydrol. 387 (3–4), 304–311.
Hampson, P.S., 2000. Water quality in the Upper Tennessee River Basin, Tennessee, North Carolina, Virginia, and Georgia, 1994–98, 1205. US Geological Survey.
Hayes, J.L., 2011. Record Floods of Greater Nashville: Including Flooding in Middle Tennessee (TN) and Western Kentucky (KY), May 1–4-2010: Service Assessment. DIANE Publishing.
Houghton, J.T., et al., 1996. Climate Change 1995: The Science of Climate Change. Working Group I, Second Assessment Report of the Intergovernmental Panel on Climate Change (IPCC). Cambridge University Press, UK.

Ingram, K., Dow, K., Carter, L., Anderson, J., 2013. Climate of the Southeast United States: Variability, Change, Impacts, and Vulnerability. Springer.
Jin, F.F., An, S.I., Timmermann, A., Zhao, J., 2003. Strong El Niño events and nonlinear dynamical heating. Geophys. Res. Lett. 30 (3), 20-1-20-1.
Karl, T.R., Melillo, J.M., Peterson, T.C., 2009. Global Climate Change Impacts in the United States. Cambridge University Press.
Kendall, M.G., 1975. Rank Correlation Methods, 4th ed. Griffin, London.
Konrad II, C.E., 1994. Moisture trajectories associated with heavy rainfall in the Appalachian region of the United States. Phys. Geogr. 15 (3), 227–248.
Lanzante, J.R., 1996. Resistant, robust and non-parametric techniques for the analysis of climate data: Theory and examples, including applications to historical radiosonde station data. Int. J. Climatol. 16 (11), 1197–1226.
Li, L., Li, W., Deng, Y., 2013. Summer rainfall variability over the Southeastern United States and its intensification in the 21st century as assessed by CMIP5 models. J. Geophys. Res. Atmos. 118 (2), 340–354.
Li, W., Li, L., Fu, R., Deng, Y., Wang, H., 2011. Changes to the North Atlantic subtropical high and its role in the intensification of summer rainfall variability in the southeastern United States. J. Clim. 24 (5).
Liang, L., Li, L., Liu, Q., 2011. Precipitation variability in Northeast China from 1961 to 2008. J. Hydrol. 404 (1), 67–76.
Liu, Q., Yang, Z., Cui, B., 2008. Spatial and temporal variability of annual precipitation during 1961–2006 in Yellow River Basin, China. J. Hydrol. 361 (3), 330–338.
Liu, Q., Yang, Z., Cui, B., Sun, T., 2009. Temporal trends of hydro-climatic variables and runoff response to climatic variability and vegetation changes in the Yiluo River basin, China. Hydrol. Process. 23 (21), 3030–3039.
Mann, H.B., 1945. Nonparametric tests against trend. Econometrica, 245–259.
Miller, B.A., Reidinger, R.B., Bank, W., 1998. Comprehensive River Basin Development: The Tennessee Valley Authority. World Bank.
Miller, W.P., Piechota, T.C., 2008. Regional analysis of trend and step changes observed in the hydroclimatic variables around the Colorado River basin. J. Hydrometeorol. 9, 1020–1034.
Nakken, M., 1999. Wavelet analysis of rainfall-runoff variability isolating climatic from anthropogenic patterns. Environ. Model. Softw. 14 (4), 283–295.
New, M., Todd, M., Hulme, M., Jones, P., 2001. Precipitation measurements and trends in the twentieth century. Int. J. Climatol. 21 (15), 1889–1922.
Novotny, E.V., Stefan, H.G., 2007. Stream flow in Minnesota: indicator of climate change. J. Hydrol. 334 (3), 319–333.
Partal, T., Kahya, E., 2006. Trend analysis in Turkish precipitation data. Hydrol. Process. 20 (9), 2011–2026.
Sen, P.K., 1968. Robustness of some nonparametric procedures in linear models. Ann. Math. Stat., 1913–1922.
Shifteh Some'e, B., Ezani, A., Tabari, H., 2012. Spatiotemporal trends and change point of precipitation in Iran. Atmos. Res. 113, 1–12.
Smith, M.J., Phillips, I.D., 2013. Winter daily precipitation variability over the East Anglian region of Great Britain and its relationship with river flow. Int. J. Climatol. 33 (9), 2215–2231.
Sneyers, R., 1990. On the Statistical Analysis of Series of Observations, World Meteorological Organization, Tech. Note No. 143, WMO No. 415.
Solomon, S., et al., 2007. Climate Change 2007: The Physical Science Basis. Working Group I, Fourth Assessment Report of the Intergovernmental Panel on Climate Change (IPCC). Cambridge University Press, UK.
Stocker, T.F., et al., 2013. Climate Change 2013: The Physical Science Basis. Working Group I, Fifth Assessment Report of the Intergovernmental Panel on Climate Change (ICPP). Cambridge University Press, UK.
Theil, H., 1950. A rank-invariant method of linear and polynomial regression analysis. Nederl. Akad. Wetensch. Series A 53, 386–392.
Torrence, C., Compo, G.P., 1998. A practical guide to wavelet analysis. Bull. Am. Meteorol. Soc. 79 (1), 61–78.
Viessman, W., Lewis, G.L., 2003. Introduction to Hydrology, 5th ed. Prentice Hall.
von Storch, H., Navarra, A., 1999. Analysis of Climate Variability: Applications of Statistical Techniques. Proceedings of an Autumn School, Commission of the European Community on Elba from October 30 to November 6, 1993, Springer, 342 p.
Wang, H., Fu, R., Kumar, A., Li, W., 2010. Intensification of summer rainfall variability in the southeastern United States during recent decades. J. Hydrometeorol. 11 (4).
Wei, F.Y., 1999. The Technologies of Statistics Diagnosis and Forecast in Modern Climate. China Meteorological Press, Beijing (in Chinese).
Westmacott, J.R., Burn, D.H., 1997. Climate change effects on the hydrologic regime within the Churchill-Nelson River Basin. J. Hydrol. 202 (1), 263–279.
Wu, H., Soh, L.-K., Samal, A., Chen, X.-H., 2008. Trend analysis of streamflow drought events in Nebraska. Water Resour. Manage. 22 (2), 145–164.
Yamamoto, R., Iwashima, T., Sange, N.K., 1986. An analysis of climate jump. J. Meteorol. Soc. Jpn. 64, 273–281.
Yang, L., Villarini, G., Smith, J.A., Tian, F., Hu, H., 2013. Changes in seasonal maximum daily precipitation in China over the period 1961–2006. Int. J. Climatol. 33 (7), 1646–1657.
Yue, S., Wang, C.Y., 2002. Applicability of prewhitening to eliminate the influence of serial correlation on the Mann–Kendall test. Water Resour. Res. 38 (6), 41–47.
Zhang, Q., Liu, C., Xu, C.-Y., Xu, Y., Jiang, T., 2006. Observed trends of annual maximum water level and streamflow during past 130 years in the Yangtze River basin, China. J. Hydrol. 324 (1), 255–265.
Zhang, X., Harvey, K.D., Hogg, W., Yuzyk, T.R., 2001. Trends in Canadian streamflow. Water Resour. Res. 37 (4), 987–998.
Zhang, X., Vincent, L.A., Hogg, W., Niitsoo, A., 2000. Temperature and precipitation trends in Canada during the 20th century. Atmosphere-Ocean 38 (3), 395–429.
Zhang, Y., et al., 2011. Analysis of impacts of climate variability and human activity on streamflow for a river basin in northeast China. J. Hydrol. 410 (3–4), 239–247.